Desalination and Water Treatment
www.deswater.com

doi: 10.5004/dwt.2020.24876

177 (2020) 176–185
February

Use of natural and effective mandarin peel in elimination of malachite green from the aqueous media: adsorption properties, kinetics and thermodynamics

Gizem Müjde Yalvaç, Bahar Bayrak*

Engineering Faculty, Department of Chemical Engineering, Atatürk University, 25240 Erzurum, Turkey, Tel. +90 442 231 45 18; email: batabek@atauni.edu.tr (B. Bayrak), Tel. +90 531 896 97 55; email: mujdeyalvac@gmail.com (G.M. Yalvaç)

Received 15 April 2019; Accepted 7 September 2019

ABSTRACT

Dye residuals in wastewaters of many industries are among the most important sources of environmental pollution. Malachite green (MG), one of these wastes, was removed by adsorbent produced by carbonization of mandarin peels. The carbonized mandarin peel (CMP) was characterized by Fourier transform infrared spectroscopy (FTIR), scanning electron microscopy (SEM), Brunauer–Emmett–Teller (BET) and zero point of charge (pHzpc). The equilibration time in the adsorption process was 150 min. When the equilibrium data were analyzed in terms of different isotherms, the most suitable isotherm was obtained to be Freundlich isotherm (R^2 = 0.997) and the maximum adsorption coefficient was found to be 357.14 mg/g. Different kinetic models were applied to experimental data for adsorption kinetics of MG on CMP, and it was observed that it fitted to pseudo-second-order kinetic model according to the R^2, Chi-squared and residual root mean square error values. When the thermodynamic parameters were examined, it was found that Gibb's free energy change was negative (≤–6.94 kJ/mol) and enthalpy change was 55.64 kJ/mol. Therefore, it was possible to mention that the adsorption process was spontaneous, endothermic and physical. In addition, the irregularity in the interface of the dye and CMP increased because the entropy was positive. CMP could be considered as a good alternative to available adsorbents used in waste disposal due to its high adsorption capacity, low cost and being environmentally friendly.

Keywords: Adsorption; Malachite green; Mandarin peel; Isotherm; Kinetics; Thermodynamics

1. Introduction

The industrial use of synthetic dyes has increased with developing technology. Dyes are commonly consumed in areas such as leather, paper, textile, paint, cosmetics and as a result of this, wastewaters of these industries include high levels of dye [1–3]. 10%–50% of the dye used in the dyeing industry is disposed as waste [4]. The environmental pollution caused by wastewater leads to toxic, mutagenic, carcinogenic and allergic effects on living systems [5]. Malachite green (MG) is a cationic dye in the triphenylmethane group. It is an effective drug used in the treatment of fish besides industrial consumption and has continued to be used over limits in numerous fish farms [6]. Hence, the MG must be effectively removed from systems that create pollution.

In the literature, there are many methods for the removal of dyes such as adsorption, filtration, ion exchange, ozone treatment, sedimentation, oxidation, and coagulation [7]. However, adsorption is the most preferred one among these methods because of its easiness of application and low cost [8]. In adsorption systems, activated carbon is generally used as an adsorbent due to the large surface area for the removal of waste [4,9]. However, since activated carbon has a very high cost, researchers have begun to investigate

* Corresponding author.

new alternative adsorbents. In particular, natural adsorbents have begun to be preferred for reasons such as low cost, effective performance and is not harmful to nature. While natural minerals such as clay, bentonite, and zeolite were used as natural adsorbents in the past [10–14], the use of agricultural wastes and industrial by-products has increased in recent times. For this purpose, materials such as pomegranate peels [2], peanut hulls [15], forest waste [16], hazelnut shells [17], walnut shells [18], orange peel [19], rice husk [20,21], almond shell [22], coffee husk [23], crushed waste clay bricks, municipal solid waste slag [24], and sugar cane bagasse [25] have been used. Thus, these structures which are waste for the environment, are considered in the cleaning of wastewater [26]. Mandarin, that is usually found in Asia and Brazil is a citrus fruit known as bergamot and tangerine [27]. Subsequent to mandarin's consumption as fruit and juice, non-commercial peel remains as waste.

Only a few low-cost agricultural waste methods have been tried for the removal of highly toxic MG from wastewaters [1,2,17,28–30]. Few researchers are using mandarin peel (MP) as adsorbent, and removal of heavy metals has usually been studied [26,31–34]. The studies using the CMP as the adsorbent has not been encountered frequently. In existing studies, adsorbent was prepared by heating at 100°C [26,34,35]. Thus, in this study, the potential feasibility of CMP as an adsorbent was investigated, and it was found that CMP was successfully used to remove the MG. The effects of different parameters on the adsorption were studied, and the isotherm, kinetics, and thermodynamics of the adsorption process were determined with this data.

2. Materials and methods

2.1. Preparation of CMP adsorbent and MG solution

The mandarin was bought from the local markets and then the collected crude peels were washed to take away the contamination and treated with the distilled water. Then, they were dried at 100°C for 24 h. The dried peels were placed in a stainless steel vessel through which nitrogen was passed at a rate of 100 mL/min, and carbonized at 850°C for 90 min. The CMP was sieved to a size between 0.4 and 0.22 mm. They were kept in glass containers to prevent contamination of moisture and other contaminants until to be used.

99% MG salt ($C_{23}H_{26}N_2Cl$) purchased from Merck (Darmstadt, Germany) was dissolved in distilled water to prepare a 1,000 mg/L stock solution.

2.2. Characterization of CMP adsorbent

FTIR (Bruker VERTEX 70v model, Germany) was used to determine the functional groups on the surface of CMP and crude mandarin peel. FTIR results were analyzed in the range of 400–4,000 cm^{-1} wavelengths.

BET, Brunauer, Emmett and Teller instrument (Micromeritics/3 Flex 4.02 model, USA) was used to determine specific surface areas of the CMP and MP with liquid nitrogen at 77 K temperature.

Surface morphologies of MP and CMP were visualized with SEM, scanning electron microscope (Zeiss, Germany/Sigma 300 model, St. Louis, MO, USA).

2.3. Adsorption studies

Adsorption experiments were carried out with an Edmund Bühler TH15/KS15 branded temperature-controlled shaker (Edmund Bühler, Germany). 50 mL of MG solution that was prepared under certain conditions (pH, adsorbent dose, temperature, MG concentration) was placed in the shaker. The samples were taken at fixed time intervals (5–150 min) to determine the contact time and then the remaining MG concentration in solution was measured by UV spectrophotometer (Thermo Electron Corporation Evolution 500 model, England) at λ_{max} = 617 nm. The adsorption experiments were carried out with parameters such as pH, adsorbent amount, stirring speed, contact time, initial solution concentration and temperature after the equilibration time was determined. The desired pH values were adjusted with 0.1 mol/L sodium hydroxide and hydrochloric acid using Hanna HI 11102 model pH meter (USA).

Adsorption capacity, q_e is the adsorbed MG amount per CMP (mg/g) and was given in the following equation.

$$q_e = \frac{C_0 - C_e}{m} \times V \quad (1)$$

C_0 and C_e are initial and equilibrium MG concentration (mg/L), respectively; V is the initial solution volume (L); m is mass of CMP (g).

The % removal of MG from solution is found by using Eq. (2).

$$\%\text{Removal} = \frac{C_0 - C_e}{C_0} \times 100 \quad (2)$$

3. Results and discussion

3.1. Characterization of CMP adsorbent

SEM images of MP, CMP, and CMP obtained after adsorption are given in Fig. 1. Fig. 1a indicates that the surface of the dried MP was quite smooth at 1 μm magnitude. Fig. 1b indicates the SEM image having the same magnitude as Fig. 1a of the CMP; very large pores due to carbonization were observed. In Fig. 1c, dye molecules filling into these pores due to adsorption are seen.

When the surface areas of MP and CMP were examined, the surface area for MP was determined to be 1.68 m^2/g and determined to be 1.76 m^2/g for CMP due to carbonization. Since the pores on the CMP filled with dye after adsorption, this value decreased to 1.13 m^2/g. Since the surface areas of organic wastes were low, pre-treatments such as chemical activation or carbonization were applied to be used as adsorbents. In a study on pomegranate peel, the area of raw pomegranate peel changed from 1.83 to 2.23 m^2/g by carbonization [2]. Similarly, it was increased up to 25.2 m^2/g by bind of zero-valent nano-iron [30].

Pectin having a lignocellulose structure was in large quantities in the structure of mandarin peel [36]. When the FTIR spectrum of the mandarin peel is examined in Fig. 2, a large peak at 3,335 cm^{-1} wavelength was seen. This peak was the OH stretching vibration peak which indicated the hydroxyl components in structures such as alcohol, phenol [2,26,37]. 2,931 cm^{-1} band gave asymmetric and symmetrical stretching vibrations

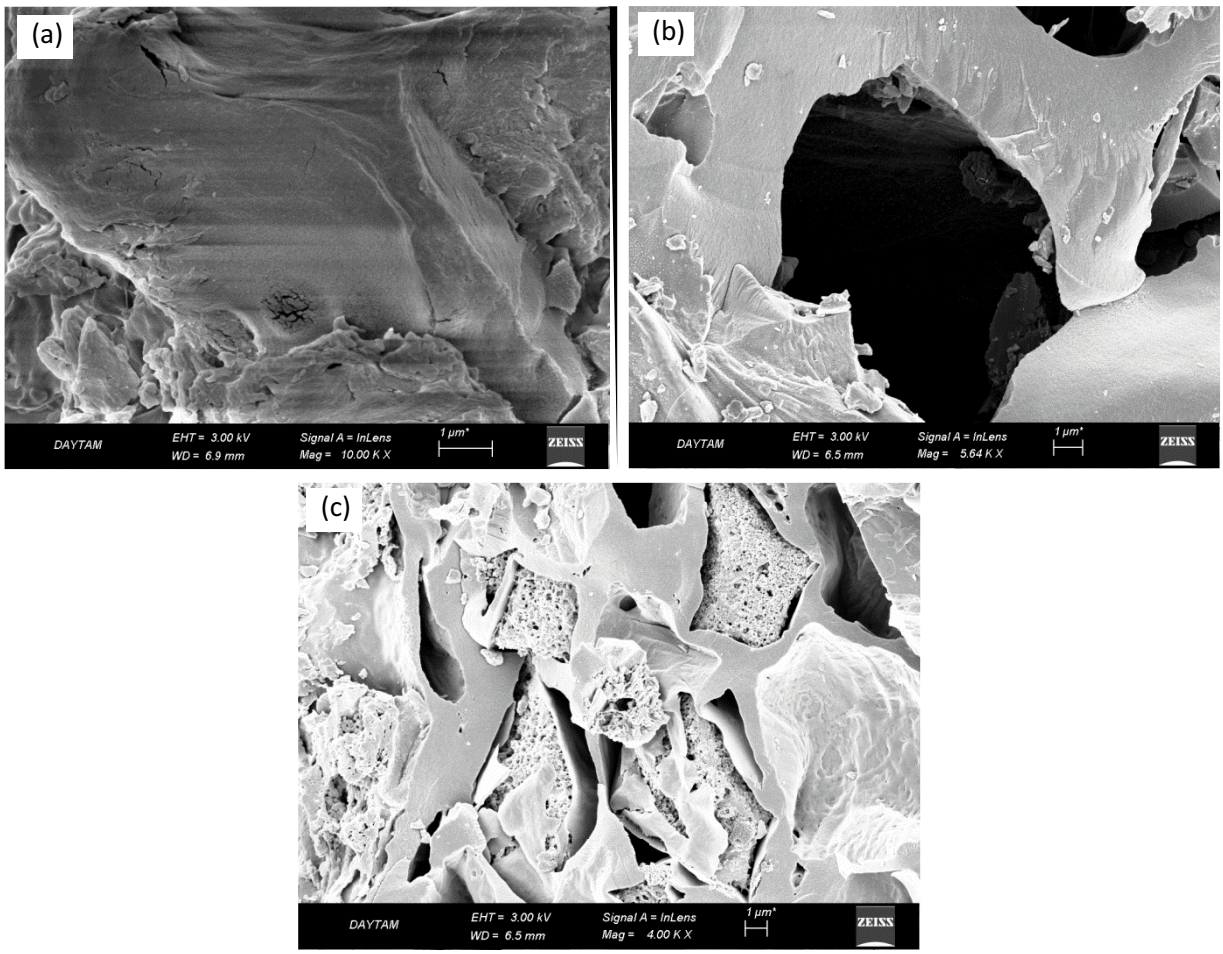

Fig. 1. SEM images of (a) crude MP, (b) CMP, and (c) CMP after adsorption.

of CH, CH_2, and CH_3 in the cellulosic structure [36,37]. While 1,734 and 2,069 cm^{-1} bands gave the C=O stretching of the carbonyl group in the carboxylic acid, 1,605 cm^{-1} peak indicated stretching vibration of C=C and C=O in aromatic ring [2,34]. The band at 1,527 cm^{-1} was due to C=O stretching of carbonyl group in primary amide [36]. C–OH in the phenolic structure caused the absorption band at 1,437 and 1,024 cm^{-1} showing C–O–C glycoside bonds in cellulosic materials [2,37].

When the mandarin peel was carbonized, the functional groups on its surface deteriorated increasing the temperature and simpler spectra were obtained [2]. 2,980 cm^{-1} band was due to the C–H stretching of aliphatic groups [38,39]. 2,868 cm^{-1} peak indicated a CH_3 group in the dye adsorbed after adsorption [40]. In Fig. 2, 2,357 and 2,355 cm^{-1} bands of CMP and CMP after adsorption indicate C=C stretching of the alkyne formed by thermal degradation [41,42]. 2,118 cm^{-1} indicated O–H stretching [2]. 1,988; 1,996 and 2,069 cm^{-1} peaks showed C=O stretching band [2]. 1,051 and 1,034 cm^{-1} gave stretching vibration of C–N groups in aliphatic amines [36]. When Fig. 2 was analyzed, it was estimated that the 1,527; 1.605 and 1,734 cm^{-1} peaks in MP shifted 1,996; 2,118 and 2,357 cm^{-1} in CMP, 1,988; 2,069 and 2,355 cm^{-1} in CMP after adsorption, respectively.

pHzpc value of adsorbent was very important for characterization. Therefore, the pHzpc value of CMP was determined with the following procedure. Firstly, a 0.01 molar sodium chloride solution was prepared, and a 50 mL solution was placed into each of 6 beakers. Then, the pH value of each solution varied from 2 to 12. 0.2 g CMP was added to each and the mixture was shaken for 10 min, kept for 24 h at 20°C. The final pH values of the solutions were measured. The difference (ΔpH) between the initial and final pH was plotted against the initial pH. pHzpc value is the point where the curve of ΔpH vs. pH_i crossed the line equal to zero [43]. The pHzpc value of CMP was obtained to be 9.6.

3.2. Effect on adsorption capacity of contact time in the different initial concentration

The adsorption data of the dye vs. the contact time for different concentrations are given in Fig. 3. While adsorption was very fast up to 60 min, it decreased to a flat plateau as time progressed. The adsorption was initially rapid because the driving force due to the high initial solution concentration destroyed the resistance between CMP with high porosity and MG [44]. Although the equilibrium time at the solid–liquid interface was shorter at lower concentrations, all experiments were carried out with a contact time of 150 min to obtain equilibrium values at higher concentrations.

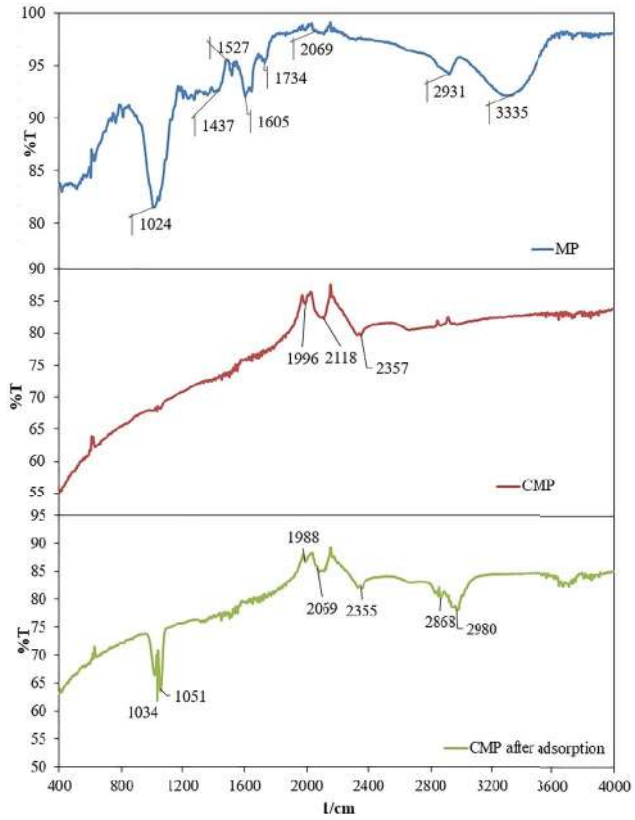

Fig. 2. FTIR spectra of MP, CMP, and CMP after adsorption.

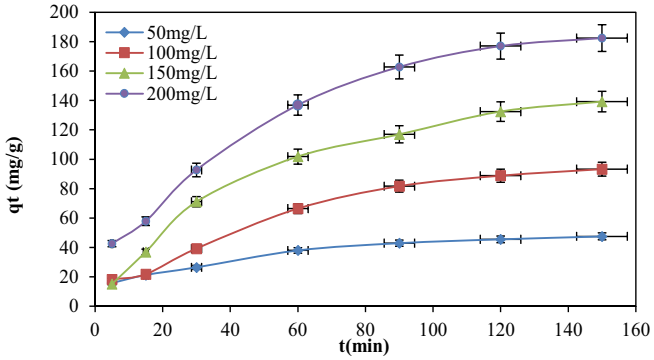

Fig. 3. Effect on q_t contact time and different initial concentration (T = 30°C, pH = 6, and adsorbent amount = 0.05 g).

3.3. Effect of CMP dosage

The change of percent removal and q_e value with increasing adsorbent dose are shown in Fig. 4. As the amount of adsorbent increased, the percentage of removal increased from 50.6 to 96.04 depending on the increase of active binding centers on areas and surface areas [45]. When more than 0.05 g adsorbent was used, the adsorption rate slowed down as the remaining dye was lower than the existing adsorption area [38]. The adsorption capacity (q_e) decreased from 379.36 to 72.03 mg/g as the amount of adsorbent was increased, due to the increase in the unsaturated surface areas [46].

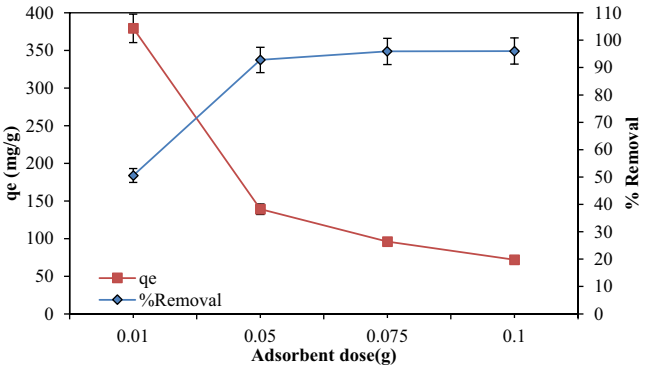

Fig. 4. Effect of adsorbent dosage (T = 30°C, pH = 6, C_0 = 150 mg/L, and t = 150 min).

3.4. Effect of MG solution temperature

Temperature is one of the most important parameters in adsorption processes. The change in temperature from 25°C to 50°C caused the % removal increased from 91.72 to 98.19, and the adsorption capacity varied from 137.58 to 147.28 mg/g (Fig. 5). This indicated that the adsorption was an endothermic nature. While the % removal change at low temperatures was less, it increased at temperatures higher than 35°C, because the increase in temperature caused the dye molecules to have more energy and thus more easily interacted with the active regions on the surface. At the same time, the temperature rise caused the formation of new active centers and larger pores due to the breakage of the bonds on the adsorption surface. Thus, the diffusion rate increased also in pores and boundary layers on the adsorbent surface [43,44].

3.5. Effect of initial concentration of MG solution

The initial concentration effect of MG on adsorption capacity and removal of the dye is shown in Fig. 6. When the concentration changed between 50 and 200 mg/L, the adsorption capacity increased from 47.5 to 182.45 mg/g, and the dye removal decreased from 95% to 91.22%. q_e value increased in parallel with the increase in concentration. Because the mass transfer resistance formed between the aqueous dye phase, and the solid CMP adsorbent was broken by increasing the initial concentration. The decrease in removal was due to the limited number of binding sites on the adsorbent despite increased dye molecules. So that competing dye molecules were difficult to bond to the surface [47,48].

3.6. Effect of pH solution

pH is a very important parameter for all adsorption processes because of its effects on the surface properties of the adsorbent and the ionization degrees of the adsorbate's functional groups [42,49]. This effect can be explained by the pHzpc value (zero point charge) of adsorbent and the pKa value of the adsorbate. The pKa value of the MG solution used as the adsorbate is 6.9 [2]. Accordingly, when the solution pH value was less than 6.9, MG behaved as anionic. Conversely, it turned cationic into pH > 6.9. The pHzpc value of CMP adsorbent was found to be 9.6. So, the adsorbent

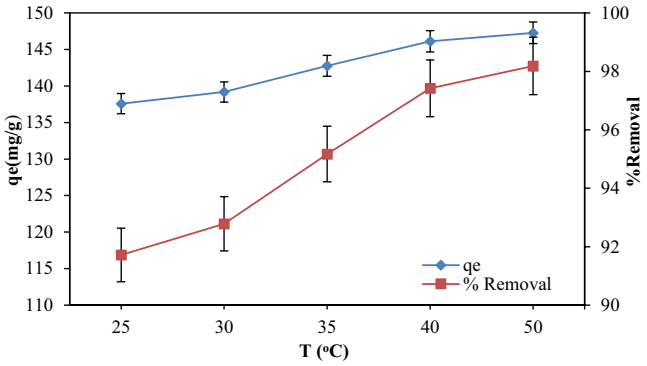

Fig. 5. Effect of MG solution temperature (adsorbent dose = 0.05 g, pH = 6, C_0 = 150 mg/L, and t = 150 min).

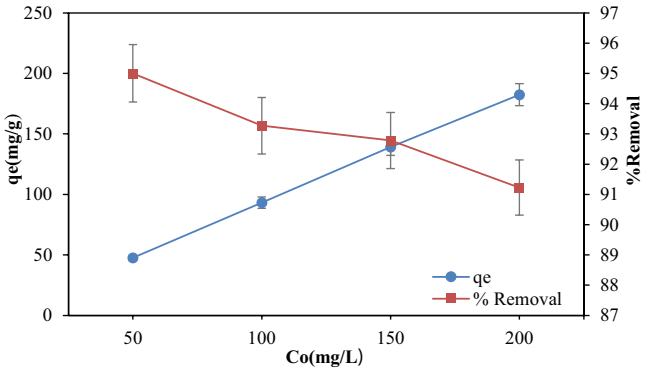

Fig. 6. Effect of initial concentration of MG solution (adsorbent dose = 0.05 g, pH = 6, T = 30°C, and t = 150 min).

acted as cationic when the solution pH was less than 9.6. The effect of pH was examined with these parameters and it was noticed that MG was anionic and CMP was cationic for the solution of pH < 6.9. Thus, electrostatic attraction occurred, and the efficiency of dye removal increased. Adsorbent and adsorbate repelled each other due to cationic in ranges between 6.9 < pH < 9.6. The % removal increased at pH values greater than 9.6 as CMP was anionic. The effect of this parameter on adsorption was examined by changing the pH from 3 to 10 in Fig. 7 and it was seen that the removal increased up to pH 6.0, did not change significantly from 94.06% at pH 6.0 to 95.35% at pH 9.0 and increased again 97.14% at pH 10 [2,50,51]. As seen in Fig. 7, while the removal efficiency and adsorption capacities were 53.95 and 80.93 mg/g at pH 2, they decreased sharply to 2.53 and 3.80 mg/g at pH 4, respectively.

It was thought that the dye decomposed at pH 2 due to the color changing from green to yellow [5,52]. The % removal and adsorption capacities at pH 4 have sharply decreased as can be seen in Fig. 7. At this pH value, the strong interaction between the adsorbent and the MG molecules could deteriorate the pore structure of the CMP. It was seen that similar results were obtained in studies using cationic dye [51–53].

3.7. Adsorption isotherms

Adsorption isotherms enabled to understand the relationship between adsorbent and adsorbate. Thus, equilibrium

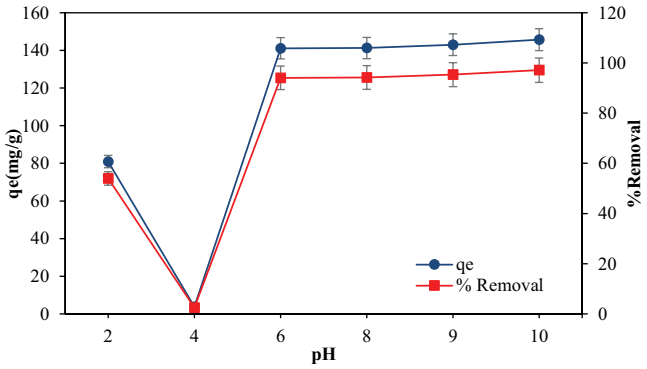

Fig. 7. Effect of initial solution pH (adsorbent dose = 0.05 g, C_0 = 150 mg/L, T = 30°C, and t = 150 min).

data were analyzed using the Langmuir, Freundlich, Temkin, Dubinin–Radushkevich, Redlich–Peterson isotherms. The linear equations and constants used for each isotherm are given in Table 1.

In the Langmuir isotherm, it was assumed that the adsorption occurred with monolayer coverage, and the adsorbent sites had homogeneous distribution on the surface. In addition, the adsorbed dye molecules did not interact with each other [54]. The dimensionless separation factor R_L was calculated using the Langmuir isotherm constants shown in Table 1.

$$R_L = \frac{1}{1 + K_L \times C_0} \tag{3}$$

It was indicated that adsorption was irreversible for R_L = 0, linear for R_L = 1 and favourable for 0 < R_L < 1 [45].

It was supposed in the Freundlich isotherm that the process happened as multilayer due to surface-active centers with different affinities on the heterogeneous surface. If n value given in Table 1 varied from 1 to 10, the adsorption was considered to be appropriate [55,59].

In the Temkin isotherm, it was deemed that the adsorption heat of all molecules decreased linearly with coverage due to interactions of adsorbent–adsorbate [56,60]. The RT/b expression in the Temkin isotherm was briefly shown as B_T. The positive B_T values indicated that the adsorption was endothermic [61].

The Polanyi potential and the mean adsorption energy (E) at Dubinin–Radushkevich (D–R) isotherm are presented in the following equations [57].

$$\varepsilon = RT \ln\left[1 + \frac{1}{C_e}\right] \tag{4}$$

$$E = \frac{1}{\sqrt{2K_{DR}}} \tag{5}$$

The E (kJ/mol) value indicated information about the adsorption process. When the obtained E value was less than 8 kJ/mol, adsorption was physical and the adsorption was the chemical nature for the E values greater than 16 kJ/mol.

Table 1
Isotherms used to analyze equilibrium data

Isotherm	Linear equation	Plot	Isotherm constants	References
Langmuir	$\frac{C_e}{q_e}=\frac{1}{q_m K_L}+\frac{C_e}{q_m}$	$\frac{C_e}{q_e}$ vs. C_e	q_m is the maximum adsorption capacity K_L is the Langmuir constant	[54]
Freundlich	$\ln q_e=\ln K_F+\frac{1}{n}\ln C_e$	$\ln q_e$ vs. $\ln C_e$	K_F is the Freundlich constant n gives the adsorption intensity	[55]
Temkin	$q_e=\frac{RT}{b}\ln K_T+\frac{RT}{b}\ln C_e$	q_e vs. $\ln C_e$	K_T is the equilibrium binding constant b is Temkin constant related to heat of adsorption	[56]
Dubinin–Radushkevich	$\ln q_e=\ln q_m-K_{\mathrm{DR}}\varepsilon^2$	$\ln q_e$ vs. ε^2	K_{DR} is the activity coefficient related to mean adsorption energy ε is Polanyi potential	[57]
Redlich–Peterson	$\ln\left(\frac{K_R C_e}{q_e}-1\right)=\beta_R\ln C_e+\ln\alpha_R$	$\ln\left(\frac{K_R C_e}{q_e}-1\right)$ vs. $\ln C_e$	K_R and α_R is R–P isotherm constant β_R is exponent of R–P isotherm	[58]

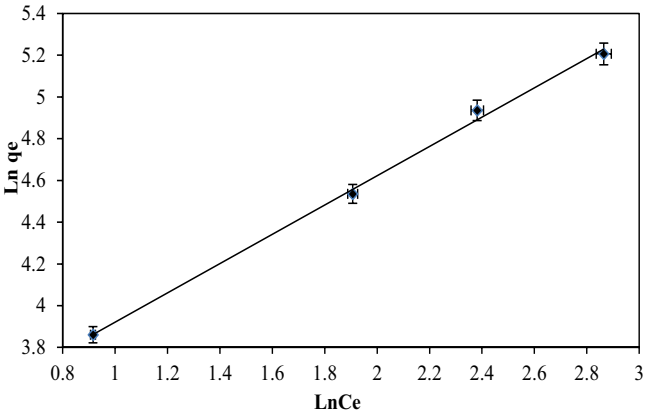

Fig. 8. Freundlich isotherm curve (adsorbent amount = 0.05 g; contact time = 150 min, pH = 6, temperature = 30°C).

E values found between 8 and 16 kJ/mol indicated that the adsorption was carried out by the ion exchange mechanism [2].

Redlich–Peterson (R–P) isotherm was a hybrid isotherm which could be applied to homogeneous and heterogeneous systems and approaches to the Langmuir (when $\beta_R = 1$) and Freundlich isotherms (when $\beta_R = 0$) depending on the β_R [58].

As can be seen in Table 2 and Fig.8, the most suitable isotherm was obtained to be Freundlich isotherm with $R^2 = 0.997$ among the applied isotherms for the adsorption of MG with CMP. As the n value at Freundlich isotherm was 1.42 g/L, and the value of R_L at Langmuir isotherm was between 0.08 and 0.258, adsorption was considered to be appropriate. The B_T value in the Temkin isotherm was obtained to be 68.72. This result implied that the adsorption was endothermic.

Table 2
Isotherm constants and the correlation coefficients of isotherm models for the adsorption of the MG onto CMP

Isotherms	Isotherm constants			
Langmuir	q_m (mg/g)	b (L/mg)	R^2	R_L
30°C	357.14	0.057	0.965	0.258
				0.148
				0.104
				0.080
Freundlich	K_F (mg/g) (L/mg)$^{1/n}$	n (g/L)	R^2	
30°C	25.00	1.42	0.997	
Temkin	B_T	K_T (L/g)	R^2	
30°C	68.72	0.715	0.966	
Dubinin–Radushkevich	q_s (mg/g)	B(mol²/J²)	R^2	E(kJ/mol)
30°C	150.07	0.000002	0.875	0.5
Redlich–Peterson	K_R (L/g)	β	R^2	α_R (L/mg)
30°C	20.49	0.465	0.986	0.764

Since the E value at the D–R isotherm was 0.5 kJ/mol which was smaller than 8 kJ/mol, adsorption was the physical adsorption. β value of 0.465 indicated that the isotherm was approaching Freundlich isotherm.

3.8. Adsorption kinetics

Adsorption kinetics were examined by the models given in Table 3 for the removal of MG using CMP [62–65].

Kinetic constants in Table 4 were obtained using the relationship between experimental data and time with the equations given in Table 3.

When Table 4 and Fig. 9 were examined to determine the kinetic model, it was found that the pseudo-second-order model, indicating the highest R^2 and lowest chi-square and residual root mean square error (RMSE) values, was the most suitable model [30].

Table 3
Kinetic models applied for adsorption

Kinetic model	Integrated equation	Model constants	References
Pseudo-first-order	$\log\left(q_e - q_t\right) = \log q_e - \frac{K_1}{2.303}t$	K_1 is pseudo-first-order rate constant	[62]
Pseudo-second-order	$\frac{t}{q_t} = \frac{1}{K_2 q_e^2} + \frac{t}{q_e}$	K_2 is second-order rate constant	[63]
Elovich	$q_t = \frac{1}{\beta}\ln\left(\alpha \times \beta\right) + \frac{1}{\beta}\ln\left(t\right)$	α and β are Elovich constants	[65]
Intra-particle diffusion	$q_t = K_i t^{\frac{1}{2}} + C$	K_i is intra-particle diffusion constant	[64]

Table 4
Kinetic constants for different kinetic model

Kinetic model	Kinetic constants					
Pseudo-first-order model	K_1 (1/min)	q_e (mg/g)	R^2	q_e (mg/g) (experimental)	Chi-square	RMSE
50 mg/L	24×10^{-3}	39.37	0.997	47.50	0.29	2.85
100 mg/L	29×10^{-3}	118.93	0.970	93.27		
150 mg/L	30×10^{-3}	185.27	0.940	139.18		
200 mg/L	33×10^{-3}	232.27	0.961	182.45		
Pseudo-second-order model	K_2 (mg/g min)	q_e (mg/g)	R^2	q_e (mg/g) (experimental)	Chi-square	RMSE
50 mg/L	8×10^{-4}	53.76	0.989	47.50	0.05	1.65
100 mg/L	1×10^{-4}	128.21	0.941	93.27		
150 mg/L	8×10^{-5}	196.08	0.995	139.18		
200 mg/L	1×10^{-4}	227.27	0.982	182.45		
Elovich model	α (mg/g min)	β (mg/g min)	R^2	Chi-square	RMSE	
50 mg/L	6.96	9.9×10^{-2}	0.962	0.18	3.15	
100 mg/L	6.27	4.0×10^{-2}	0.926			
150 mg/L	8.99	2.6×10^{-2}	0.982			
200 mg/L	15.82	2.2×10^{-2}	0.955			
Intra-particle diffusion model	K_i (mg/g min^2)	C	R^2	Chi-square	RMSE	
50 mg/L	3.37	8.88	0.977	1.93	12.15	
100 mg/L	2.23	–4.14	0.973			
150 mg/L	2.70	–6.78	0.975			
200 mg/L	3.24	8.43	0.977			

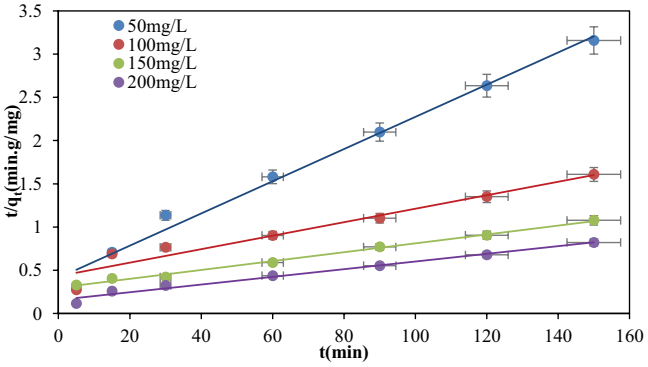

Fig. 9. Pseudo-second-order model (conditions: contact time = 150 min, pH = 6, dose of adsorbent = 0.05 g, and temperature = 30°C).

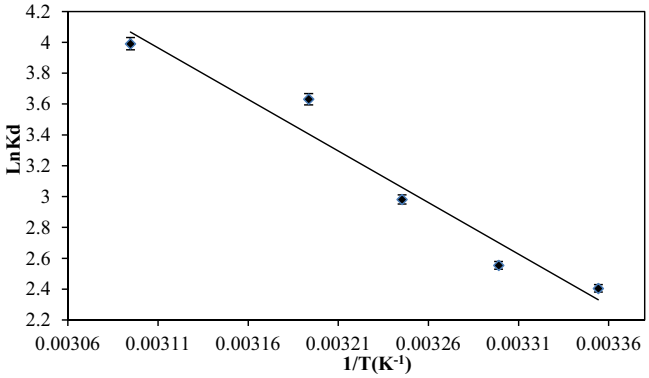

Fig. 10. Plot of the Van't Hoff equation.

3.9. Adsorption thermodynamics

The adsorption thermodynamics were determined by the parameters of $\Delta G°$ (kJ/mol), $\Delta H°$ (kJ/mol), $\Delta S°$ (kJ/mol K) and $\Delta G°$ was obtained with Eq. (6).

$$\Delta G° = -RT \ln K_D \quad (6)$$

where R was 8.314 J/mol K, T (K) indicated the temperature and K_D was the distribution coefficient indicating the affinity of the adsorbent surface. The distribution coefficient was calculated with Eq. (7).

$$K_D = \frac{q_e}{C_e} \quad (7)$$

The parameters of $\Delta H°$ and $\Delta S°$ were determined with Van't Hoff Eq. (8) using the distribution coefficient and the slope and intersection values of $1/T$ graph against $\ln K_D$ (Fig. 10) [2,30,44].

$$\ln K_D = \frac{\Delta S°}{R} - \frac{\Delta H°}{RT} \quad (8)$$

Table 5
Thermodynamics constants

T (K)	$\Delta H°$ (kJ/mol)	$\Delta S°$ (kJ/mol K)	$\Delta G°$ (kJ/mol)
298			–6.94
303			–7.99
308	55.64	0.21	–9.04
313			–10.09
318			–12.19

The value of $\Delta H°$ was positive, therefore the adsorption process was carried out endothermically as seen in Table 5 [2]. The $\Delta G°$ value varied from –6.94 to –12.19 kJ/mol with increasing temperature. This indicated that the adsorption happened spontaneously. Since the $\Delta G°$ values were greater than –20 kJ/mol, it was possible to mention that the adsorption occurred as physical [16,30], The $\Delta S°$ value of 0.21 kJ/mol K, showed that degree of disorder in the interface of the CMP adsorbent and MG solution increased.

3.10. Comparison of adsorbents used for the removal of MG

Many adsorbents have been used for the removal of MG. CMP and the adsorbents obtained from various organic wastes are compared in Table 6. It was found that the

Table 6
Comparison of adsorbents obtained from organic waste used for removal of MG

Adsorbents	q_m (mg/g)	Equilibrium time	pH	Adsorbent dose	References
Oat hull	83.0	80 min	8	2.5 g/L	[1]
Carbonized pomegranate peel	31.45	90 min	5	0.1 g/L	[2]
Chemically modified rice husk	15.49	120 min	7.0	1.0 g/L	[28]
Citrus limetta peel	8.73	30 min	7	0.5 g/L	[42]
Zea mays cob	16.72	30 min	7	0.5 g/L	[42]
Rambutan peel-based activated carbon	329.49	24 h	8	0.2 g/L	[44]
Breadnut peel	180.00	240 min	8.02	–	[66]
Lemon peel	51.73	24 h	–	0.5 g/L	[67]
Eggshells	243.20	180 min	6	1.0 g/L	[68]
Jatropha curcas L.	21.78	180 min	6	4.0 g/L	[69]
CMP	357.14	150 min	6	1 g/L	In this study

adsorption capacity of the CMP was quite high for the lower adsorbent dosage and the equilibration time when compared with the pre-treated adsorbents (Table 6).

4. Conclusion

In this study, the effect of CMP as an adsorbent produced with carbonization from the mandarin peel in the removal of MG, which is frequently encountered in the wastes of the industries where dye is used was investigated. The surface properties of CMP were characterized by FTIR, SEM, BET and pHzpc analyses. When the experimental data were applied to the adsorption isotherm models, the best fit model was found to be Freundlich isotherm. Maximum adsorption capacity according to Langmuir isotherm was determined to be 357.14 mg/g. Experimental studies to determine the mechanism of adsorption were applied to different kinetic models, and both error analyses and R^2 values were examined, and it was decided to be a pseudo-second-order. Thermodynamic data revealed that adsorption was endothermic, and the physical process and degrees of disorder in the solid–liquid interface increased. CMP could be used as an adsorbent in the industry due to its high adsorption capacity, high removal efficiency, it is being environmentally friendly, cheap and easy to find.

Acknowledgment

The authors would like to thank the Atatürk University Research Foundation (Project No: 2016/185) for supporting this study financially.

References

[1] S. Banerjee, G.C. Sharma, R.K. Gautam, M.C. Chattopadhyaya, S.N. Upadhyay, Y.C. Sharma, Removal of Malachite Green, a hazardous dye from aqueous solutions using *Avena sativa* (oat) hull as a potential adsorbent, J. Mol. Liq., 213 (2016) 162–172.
[2] F. Gündüz, B. Bayrak, Biosorption of malachite green from an aqueous solution using pomegranate peel: equilibrium modelling, kinetic and thermodynamic studies, J. Mol. Liq., 243 (2017) 790–798.
[3] M.R.R. Kooh, M.K. Dahri, L.B.L. Lim, L.H. Lim, O.A. Malik, Batch adsorption studies of the removal of methyl violet 2B by soya bean waste: isotherm, kinetics and artificial neural network modelling, Environ. Earth Sci., 75 (2016) 783.
[4] Y.S. Al-Degs, M.I. El-Barghouthi, A.H. El-Sheikh, G.M. Walker, Effect of solution pH, ionic strength, and temperature on adsorption behavior of reactive dyes on activated carbon, Dyes Pigm., 77 (2008) 16–23.
[5] Y. Song, S. Ding, S. Chen, H. Xu, Y. Mei, J. Ren, Removal of malachite green in aqueous solution by adsorption on sawdust, Korean J. Chem. Eng., 32 (2015) 2443–2448.
[6] T. Kobayashi, H. Taya, P. Wilaipun, W. Chinaksorn, K. Yonezuka, T. Harada, W. Ishida, H. Yano, T. Terahara, C. Imada, M. Kamio, Malachite-green-removing properties of a bacterial strain isolated from fish ponds in Thailand, Fish. Sci., 83 (2017) 827–835.
[7] V. Gupta, Application of low-cost adsorbents for dye removal – a review, J. Environ. Manage., 90 (2009) 2313–2342.
[8] F. Jiang, D.M. Dinh, Y.-L. Hsieh, Adsorption and desorption of cationic malachite green dye on cellulose nanofibril aerogels, Carbohydr. Polym., 173 (2017) 286–294.
[9] Y.S. Al-Degs, M.A.M. Khraisheh, S.J. Allen, M.N. Ahmad, Adsorption characteristics of reactive dyes in columns of activated carbon, J. Hazard. Mater., 165 (2009) 944–949.
[10] M.K. Uddin, A review on the adsorption of heavy metals by clay minerals, with special focus on the past decade, Chem. Eng. J., 308 (2017) 438–462.
[11] V. Hovhannisyan, C.-Y. Dong, S.-J. Chen, Photodynamic dye adsorption and release performance of natural zeolite, Sci. Rep.-UK, 7 (2017) 45503.
[12] L. Deng, P. Yuan, D. Liu, F. Annabi-Bergaya, J. Zhou, F. Chen, Z. Liu, Effects of microstructure of clay minerals, montmorillonite, kaolinite and halloysite, on their benzene adsorption behaviors, Appl. Clay Sci., 143 (2017) 184–191.
[13] O. Korkut, E. Sayan, O. Lacin, B. Bayrak, Investigation of adsorption and ultrasound assisted desorption of lead (II) and copper (II) on local bentonite: a modelling study, Desalination, 259 (2010) 243–248.
[14] O. Lacin, B. Bayrak, O. Korkut, E. Sayan, Modeling of adsorption and ultrasonic desorption of cadmium(II) and zinc(II) on local bentonite, J. Colloid Interface Sci., 292 (2005) 330–335.
[15] N. Tahir, H.N. Bhatti, M. Iqbal, S. Noreen, Biopolymers composites with peanut hull waste biomass and application for Crystal Violet adsorption, Int. J. Biol. Macromol., 94 (2017) 210–220.
[16] A. Bouguettoucha, A. Reffas, D. Chebli, A. Amrane, Adsorption of the cationic dye ethyl violet on acid and alkali-treated wild carob powder, a low-cost adsorbent derived from forest waste, Iran. J. Chem. Eng., 36 (2017) 87–96.
[17] J. Shuang, L. Linlin, W. Pingping, G. Hongwei, Study on the adsorption of Pb(II) and methylene blue and malachite green by chemically modified hazelnut shell powder, Shandong Chem. Ind., 10 (2017) 74.
[18] R. Tang, C. Dai, C. Li, W. Liu, S. Gao, C. Wang, Removal of methylene blue from aqueous solution using agricultural residue walnut shell: equilibrium, kinetic, and thermodynamic studies, J. Chem., 2017 (2017), https://doi.org/10.1155/2017/8404965.
[19] M. Arami, N.Y. Limaee, N.M. Mahmoodi, N.S. Tabrizi, Removal of dyes from colored textile wastewater by orange peel adsorbent: equilibrium and kinetic studies, J. Colloid Interface Sci., 288 (2005) 371–376.
[20] I. Anastopoulos, G.Z. Kyzas, Agricultural peels for dye adsorption: a review of recent literature, J. Mol. Liq., 200 (2014) 381–389.
[21] V. Vadivelan, K.V. Kumar, Equilibrium, kinetics, mechanism, and process design for the sorption of methylene blue onto rice husk, J. Colloid Interface Sci., 286 (2005) 90–100.
[22] D. Ozdes, A. Gundogdu, C. Duran, H.B. Senturk, Evaluation of adsorption characteristics of malachite green onto almond shell (*Prunus dulcis*), Sep. Sci. Technol., 45 (2010) 2076–2085.
[23] T.P.K. Murthy, B.S. Gowrishankar, M.N.C. Prabha, M. Kruthi, R.H. Krishna, Studies on batch adsorptive removal of malachite green from synthetic wastewater using acid treated coffee husk: equilibrium, kinetics and thermodynamic studies, Microchem. J., 146 (2019) 192–201.
[24] G.M.P. Kumara, K. Kawamoto, Applicability of crushed clay brick and municipal solid waste slag as low-cost adsorbents to refine high concentrate Cd (II) and Pb (II) contaminated wastewater, Int. J. GEOMATE, 17 (2019) 133–142.
[25] A.O.A. El Naga, M. El Saied, S.A. Shaban, F.Y. El Kady, Fast removal of diclofenac sodium from aqueous solution using sugar cane bagasse-derived activated carbon, J. Mol. Liq., 285 (2019) 9–19.
[26] A. Abdolali, H.H. Ngo, W. Guo, S. Lu, S.-S. Chen, N.C. Nguyen, X. Zhang, J. Wang, Y. Wu, A breakthrough biosorbent in removing heavy metals: equilibrium, kinetic, thermodynamic and mechanism analyses in a lab-scale study, Sci. Total Environ., 542 (2016) 603–611.
[27] G.C. Ribeiro, L.M. Coelho, E. Oliveira, N.M.M. Coelho, Removal of Cu(II) from ethanol fuel using mandarin peel as biosorbent, BioResources, 8 (2013) 3309–3321.
[28] S. Chowdhury, R. Mishra, P. Saha, P. Kushwaha, Adsorption thermodynamics, kinetics and isosteric heat of adsorption of malachite green onto chemically modified rice husk, Desalination, 265 (2011) 159–168.
[29] J. Zhang, Y. Li, C. Zhang, Y. Jing, Adsorption of malachite green from aqueous solution onto carbon prepared from Arundo donax root, J. Hazard. Mater., 150 (2008) 774–782.

[30] F. Gündüz, B. Bayrak, Synthesis and performance of pomegranate peel-supported zero-valent iron nanoparticles for adsorption of malachite green, Desal. Wat. Treat, 110 (2018) 180–192.
[31] D.Z. Husein, Adsorption and removal of mercury ions from aqueous solution using raw and chemically modified Egyptian mandarin peel, Desal. Wat. Treat, 51 (2013) 6761–6769.
[32] C.S. Inagaki, T. de Oliveira Caretta, R.V. da Silva Alfaya, A.A. da Silva Alfaya, Mexerica mandarin (*Citrus nobilis*) peel as a new biosorbent to remove Cu(II), Cd(II), and Pb(II) from industrial effluent, Desal. Wat. Treat, 51 (2013) 5537–5546.
[33] H.N. Bhatti, I.I. Bajwa, M.A. Hanif, I.H. Bukhari, Removal of lead and cobalt using lignocellulosic fiber derived from *Citrus reticulata* waste biomass, Korean J. Chem. Eng., 27 (2010) 218–227.
[34] F.A. Pavan, I.S. Lima, É.C. Lima, C. Airoldi, Y. Gushikem, Use of Ponkan mandarin peels as biosorbent for toxic metals uptake from aqueous solutions, J. Hazard. Mater., 137 (2006) 527–533.
[35] M. Ajmal, R.A.K. Rao, R. Ahmad, J. Ahmad, Adsorption studies on *Citrus reticulata* (fruit peel of orange): removal and recovery of Ni(II) from electroplating wastewater, J. Hazard. Mater., 79 (2000) 117–131.
[36] A. Abdolali, H.H. Ngo, W. Guo, J.L. Zhou, B. Du, Q. Wei, X.C. Wang, P.D. Nguyen, Characterization of a multi-metal binding biosorbent: chemical modification and desorption studies, Bioresour. Technol., 193 (2015) 477–487.
[37] R. Rehman, M. Salman, T. Mahmud, F. Kanwal, W. Zaman, Utilization of chemically modified *Citrus reticulata* peels for biosorptive removal of Acid Yellow-73 dye from water, J. Chem. Soc. Pak, 35 (2013) 611–617.
[38] M. Ghaedi, H. Tavallali, M. Sharifi, S.N. Kokhdan, A. Asghari, Preparation of low cost activated carbon from Myrtus communis and pomegranate and their efficient application for removal of Congo red from aqueous solution, Spectrochim. Acta, Part A, 86 (2012) 107–114.
[39] A. Reffas, A. Bouguettoucha, D. Chebli, A. Amrane, Adsorption of ethyl violet dye in aqueous solution by forest wastes, wild carob, Desal. Wat. Treat, 57 (2016) 9859–9870.
[40] Ç.Ö. Ay, A.S. Özcan, Y. Erdoğan, A. Özcan, Characterization of Punica granatum L. peels and quantitatively determination of its biosorption behavior towards lead(II) ions and Acid Blue 40, Colloids Surf., B, 100 (2012) 197–204.
[41] S. Ben-Ali, I. Jaouali, S. Souissi-Najar, A. Ouederni, Characterization and adsorption capacity of raw pomegranate peel biosorbent for copper removal, J. Cleaner Prod., 142 (2017) 3809–3821.
[42] H. Singh, G. Chauhan, A.K. Jain, S.K. Sharma, Adsorptive potential of agricultural wastes for removal of dyes from aqueous solutions, J. Environ. Chem. Eng., 5 (2017) 122–135.
[43] K. Saeed, M. Ishaq, S. Sultan, I. Ahmad, Removal of methyl violet 2-B from aqueous solutions using untreated and magnetite-impregnated almond shell as adsorbents, Desal. Wat. Treat, 57 (2016) 13484–13493.
[44] M.A. Ahmad, R. Alrozi, Removal of malachite green dye from aqueous solution using rambutan peel-based activated carbon: equilibrium, kinetic and thermodynamic studies, Chem. Eng. J., 171 (2011) 510–516.
[45] M. Ghasemi, S. Mashhadi, M. Asif, I. Tyagi, S. Agarwal, V.K. Gupta, Microwave-assisted synthesis of tetraethylenepentamine functionalized activated carbon with high adsorption capacity for Malachite green dye, J. Mol. Liq., 213 (2016) 317–325.
[46] H. Shayesteh, A. Rahbar-Kelishami, R. Norouzbeigi, Adsorption of malachite green and crystal violet cationic dyes from aqueous solution using pumice stone as a low-cost adsorbent: kinetic, equilibrium, and thermodynamic studies, Desal. Wat. Treat, 57 (2016) 12822–12831.
[47] S. Banerjee, R.K. Gautam, A. Jaiswal, P.K. Gautam, M.C. Chattopadhyaya, Study on adsorption behavior of Acid Orange 10 onto modified wheat husk, Desal. Wat. Treat, 57 (2016) 12302–12315.
[48] A. Nath, S. Chakraborty, C. Bhattacharjee, Bioadsorbtion of industrial dyes from aqueous solution onto water hyacinth (*Eichornia crassipes*): equilibrium, kinetic, and sorption mechanism study, Desal. Wat. Treat, 52 (2014) 1484–1494.
[49] B. Jeyagowri, R.T. Yamuna, Potential efficacy of a mesoporous biosorbent *Simarouba glauca* seed shell powder for the removal of malachite green from aqueous solutions, Desal. Wat. Treat, 57 (2016) 11326–11336.
[50] B. Kumar, U. Kumar, Adsorption of malachite green in aqueous solution onto sodium carbonate treated rice husk, Korean J. Chem. Eng., 32 (2015) 1655–1666.
[51] S.E. Subramani, N. Thinakaran, Isotherm, kinetic and thermodynamic studies on the adsorption behaviour of textile dyes onto chitosan, Process Saf. Environ. Prot., 106 (2017) 1–10.
[52] C.-K. Lee, S.-S. Liu, L.-C. Juang, C.-C. Wang, K.-S. Lin, M.-D. Lyu, Application of MCM-41 for dyes removal from wastewater, J. Hazard. Mater., 147 (2007) 997–1005.
[53] P. Monash, G. Pugazhenthi, Adsorption of crystal violet dye from aqueous solution using mesoporous materials synthesized at room temperature, Adsorption, 15 (2009) 390–405.
[54] I. Langmuir, The adsorption of gases on plane surfaces of glass, mica and platinum, J. Am. Chem. Soc., 40 (1918) 1361–1403.
[55] H.M.F. Freundlich, Over the adsorption in solution, J. Phys. Chem., 57 (1906) 1100–1107.
[56] M.J. Temkin, V. Pyzhev, Recent modifications to Langmuir isotherms, Acta. Physiochem., 1940.
[57] M.M. Dubinin, L.V. Radushkevich, The equation of the characteristic curve of activated charcoal, Proc. Acad. Sci. Phys. Chem. Sec., USSR55, 331–333 (1947) 875–890.
[58] O. Redlich, D.L. Peterson, A useful adsorption isotherm, J. Phys. Chem., 63 (1959) 1024–1024.
[59] W. Konicki, M. Aleksandrzak, D. Moszyński, E. Mijowska, Adsorption of anionic azo-dyes from aqueous solutions onto graphene oxide: equilibrium, kinetic and thermodynamic studies, J. Colloid Interface Sci., 496 (2017) 188–200.
[60] T.A. Khan, S. Dahiya, E.A. Khan, Removal of direct red 81 from aqueous solution by adsorption onto magnesium oxide-coated kaolinite: isotherm, dynamics and thermodynamic studies, Environ. Prog. Sustainable Energy, 36 (2017) 45–58.
[61] M.A. Ahmad, N. Ahmad, O.S. Bello, Modified durian seed as adsorbent for the removal of methyl red dye from aqueous solutions, Appl. Water Sci., 5 (2015) 407–423.
[62] S. Langergren, B. Svenska, Zur theorie der sogenannten adsorption geloester stoffe, Veternskapsakad Handlingar, 24 (1898) 1–39.
[63] Y.-S. Ho, G. McKay, Pseudo-second order model for sorption processes, Process Biochem., 34 (1999) 451–465.
[64] W.J. Weber, J.C. Morris, Kinetics of adsorption on carbon from solution, J. Sanitary Eng. Div., 89 (1963) 31–60.
[65] S.H. Chien, W.R. Clayton, Application of Elovich equation to the kinetics of phosphate release and sorption in soils, Soil Sci. Soc. Am. J., 44 (1980) 265–268.
[66] H.I. Chieng, L.B. Lim, N. Priyantha, Enhancing adsorption capacity of toxic malachite green dye through chemically modified breadnut peel: equilibrium, thermodynamics, kinetics and regeneration studies, Environ. Technol., 36 (2015) 86–97.
[67] K.V. Kumar, Optimum sorption isotherm by linear and non-linear methods for malachite green onto lemon peel, Dyes Pigm., 74 (2007) 595–597.
[68] D. Podstawczyk, A. Witek-Krowiak, K. Chojnacka, Z. Sadowski, Biosorption of malachite green by eggshells: mechanism identification and process optimization, Bioresour. Technol., 160 (2014) 161–165.
[69] M. Mohammad, S. Maitra, B.K. Dutta, Comparison of activated carbon and physic seed hull for the removal of malachite green dye from aqueous solution, Water Air Soil Pollut., 229 (2018) 45.